Biosensors and Bioelectronics 166 (2020) 112399

Contents lists available at ScienceDirect

Biosensors and Bioelectronics

journal homepage: http://www.elsevier.com/locate/bios

Electrical impedance-based contractile stress measurement of human iPSC-Cardiomyocytes

Xian Wang [a,1], Li Wang [a,b,1], Wenkun Dou [a], Zongjie Huang [a], Qili Zhao [a], Manpreet Malhi [c], Jason T. Maynes [c,d,*], Yu Sun [a,e,f,g,**]

[a] Department of Mechanical and Industrial Engineering, University of Toronto, Toronto, M5S 3G8, Canada
[b] School of Mechanical & Automotive Engineering, Qilu University of Technology (Shandong Academy of Sciences), Jinan, 250353, China
[c] Department of Anesthesia and Pain Medicine and Program in Molecular Medicine, Hospital for Sick Children, Toronto, M5G 1X8, Canada
[d] Department of Biochemistry, University of Toronto, Toronto, M5S 1A8, Canada
[e] Institute of Biomaterials and Biomedical Engineering, University of Toronto, Toronto, M5S 3G9, Canada
[f] Department of Electrical and Computer Engineering, University of Toronto, Toronto, M5S 3G4, Canada
[g] Department of Computer Science, University of Toronto, Toronto, M5T 3A1, Canada

ARTICLE INFO

Keywords:
Electrical impedance
Contractile stress
Human iPSC-Cardiomyocytes
Atomic force microscopy
Mechanotransduction

ABSTRACT

Heart failure fundamentally results from loss of cardio myocyte contractility. Developing new methods that quantify the contractile stress of the human cardiomyocyte would facilitate the study of the molecular mechanism of heart failure and advance therapy development, to improve the current five year survival for these patients. The measurement of cellular electrical impedance measurement was recently applied to monitor cardiomyocyte beating rate and rhythm, for the study at cellular maturation, and for drug screening. However, due to the lack of a quantified relationship between the impedance signal and contractile stress, change of cardiomyocyte contractile stress cannot genuinely be quantified from impedance measurements. Here, we report the first quantitative relationship between contractile stress and impedance, which enables the accurate prediction of cardiomyocyte contractility using impedance signals. Through simultaneous measurement of beating human iPSC-cardiomyocytes using impedance spectroscopy and atomic force microscopy, a power-law relationship between impedance and contractile stress was established with a confidence level of 95%. The quantitative relationship was validated using pharmacology known to alter cardiomyocyte contractility and beating (verapamil, using clinically relevant concentrations of 0.05 μM, 0.10 μM, and 0.15 μM). The contractile stress values as measured by AFM were 9.04 ± 0.14 kPa (0.05 μM), 7.72 ± 0.11 kPa (0.10 μM) and 6.23 ± 0.17 kPa (0.15 μM), and as predicted by impedance using the derived power-law relationship were 9.39 kPa, 7.76 kPa, and 6.05 kPa with a relative error of 3.73%. Our power-law relationship is the first to describe a quantitative correlation between contractile stress and impedance, broadening the application of electrical impedance measurement for characterizing complex cardiac functions (beating rate, beating rhythm and contractile stress).

1. Introduction

Rhythmic contraction of cardiomyocytes is responsible for pumping oxygen-rich blood to the organs and tissues of the body. To accomplish this crucial function, cardiomyocytes utilize structurally ordered force-generating filaments that produce cellular and (through alignment) microscopic organ contractile stress (Gaitas et al., 2015; Brette et al., 2017; Ribeiro et al., 2020; Rudolph et al., 2019). Decline of the contractile function leads to heart failure, the single largest cause of morbidity and mortality in the developed countries (Hassanabad et al., 2019). The continued poor outcomes for heart failure patients, in part, results from a lack of pharmacology that can directly improve cardiomyocyte contractility (Green et al., 2016; Gorski et al., 2015; Sant'Anna et al., 2020). Developing pre-clinical models that emulate human cardiomyocyte and cardiac tissue function is important to understanding heart failure physiology and to evaluate new agents for their ability to

* Corresponding author. Department of Anesthesia and Pain Medicine and Program in Molecular Medicine, Hospital for Sick Children, Toronto, M5G 1X8, Canada.
** Corresponding author. Department of Mechanical and Industrial Engineering, University of Toronto, Toronto, M5S 3G8, Canada.
E-mail addresses: xianjeremy.wang@mail.utoronto.ca (X. Wang), jason.maynes@sickkids.ca (J.T. Maynes), sun@mie.utoronto.ca (Y. Sun).
[1] These authors contributed equally to this work.

https://doi.org/10.1016/j.bios.2020.112399
Received 5 February 2020; Received in revised form 7 May 2020; Accepted 16 June 2020
Available online 12 July 2020

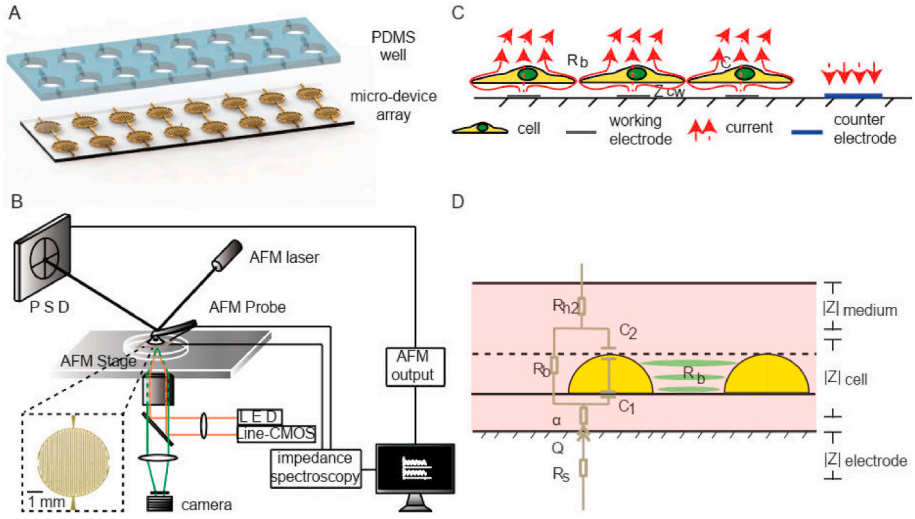

Fig. 1. (A) Micro-device array with microelectrodes for impedance-based measurement of iPSC-cardiomyocyte beating. (B) The system used in experiments integrated AFM with impedance spectroscopy for simultaneously measurement of contractile stress and impedance. (C) Electrical current flows along two paths in the microdevice cultured with cells: extracellular current flows from the microdevice surface underneath the cell, through the intercellular gap, into the culture medium (solid red line); trans-cellular current crosses the plasma membranes and cytoplasm (dashed red line). C represents the capacitance of the cell membrane R_b represents intercellular resistance. Z_{cw} represents the impedance between the bottom surface of the cell and the microdevice surface. (D) Schematic of the physical model used to extract cell parameters from impedance spectrum. C_1 and C_2 stand for the capacitance of lower and upper cell membrane. (For interpretation of the references to colour in this figure legend, the reader is referred to the Web version of this article.)

improve cardiomyocyte contractility (inotropes) (Liu et al., 2012).

As cardiomyocyte actin is dynamics, with important short-term and long-term variation after drug exposure, end-point analysis (such as α-actinin staining of fixed tissue) is less informative (Jacot et al., 2008; Bildyug and Khaitlina, 2019). End-point analysis is also generally lower throughput, hindering the evaluation of a large number of potential therapeutics. Although label-based measurement using green fluorescent protein (GFP)-tagged proteins and fluorescent calcium dyes can overcome the end-point limitation, photobleaching limits their application to recording dynamic contractility with significant reactive oxygen species generation and cell death overtime. For instance, when GFP was incorporated into β-actin filaments (GFP–β-actin) to examine the contractility of neonatal rat cardiomyocytes, significant photobleaching occurred within 18 s of measurement (Skwarek-Maruszewska et al., 2009).

In comparsion, label-free electrical impedance measurement is commonly used for sensing cell behavior changes (e.g., shape changes) (Bürgel et al., 2015; Fan et al., 2019; Giaever and Keese, 1984; Wegener et al., 2000; Zhou et al., 2016), and has been applied to the measurement of cardiomyocyte beating (Xiao et al., 2010; Scott et al., 2014; Tsai and Wang, 2016). Impedance-based devices contain micro-scale electrodes as a platform for cell growth. Physiological changes of cells (e.g., cell shape; inflow and outflow of ions) alter the electrical current between electrodes, resulting in impedance changes. Compared to fluorescent labeling, the impedance method enables label-free, long-term recording of cellular signals (Pauwelyn et al., 2015; Qiu et al., 2009). Human induced pluripotent stem cell-derived cardiomyocytes (iPSC-CM) and rat neonatal cardiomyocytes were evaluated by impedance recording including the testing of pharmaceuticals and compounds known to affect cardiomyocyte beating rate, rhythm and contractility, producing results consistent with the known cellular targets of the compounds (Scott et al., 2014). Present impedance-based measurement commonly uses the metric, termed *cell index* ($|Z_x| - |Z_0|$)/ $|Z_0|$ (Wang et al., 2013; Ke et al., 2011; Li et al., 2016), where $|Z_x|$ is the impedance magnitude measured in the presence of cells, and $|Z_0|$ is the baseline cell-free impedance magnitude. While cell index is useful to measure temporal and dynamic changes in impedance, useful for beating rate and rhythms, it is less consistent after changes to cell contractility overtime. Cell index is also strongly electrode geometry dependent, varying with microelectrode number and size and does not genuinely quantify the contractile stress generated by cardiomyocytes. As such, impedance measurement devices have more commercially been used to quantify drug-induced arrhythmia, and less for the evaluation of compounds that alter contractility.

To expand the utility of impedance measurement, capitalizing on the label-free and long-term measurement ability of the technique, we designed and fabricated a microdevice array with interdigitated electrodes (Fig. 1A). In each well, iPSC-CMs were cultured on top of the

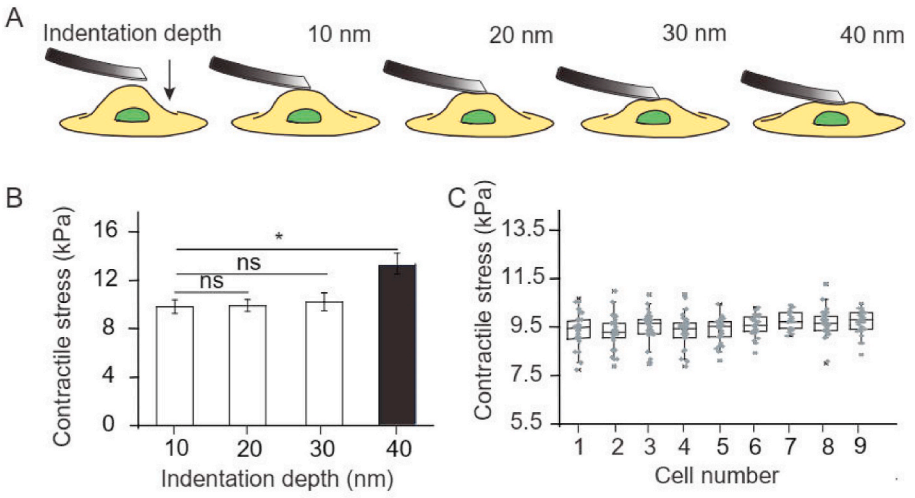

Fig. 2. (A) Schematic showing a tip-less AFM probe in contact with cells by different indentation depths (10 nm, 20 nm, 30 nm, 40 nm) during measurement. (B) Contractile stress generated by iPSC-CMs was measured by AFM under different indentation depths. The contractile stress differs significantly with indentation depth of 40 nm, n = 9 cells, *P < 0.0001, error bar: standard deviation. (C) Contractile stress distribution of 9 cells at different locations in a monolayer of iPSC-CMs, indentation depth: 10 nm. Error bar: standard deviation.

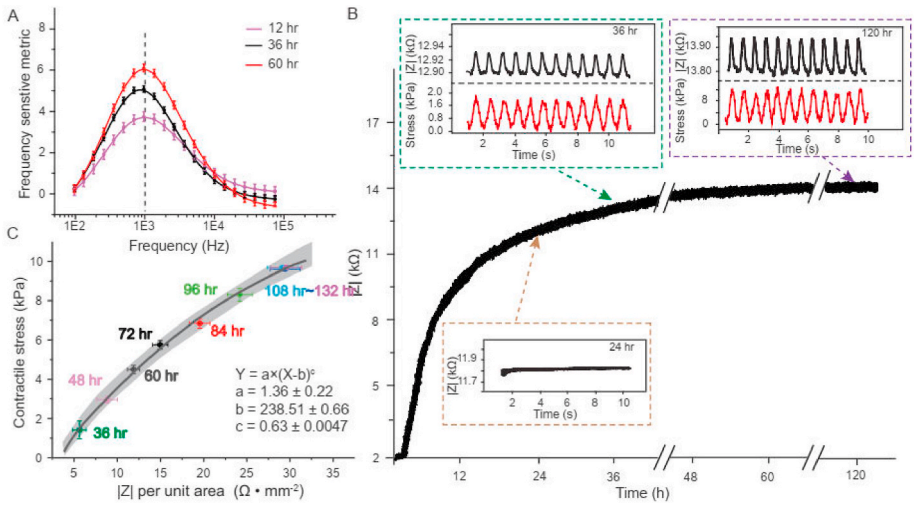

Fig. 3. (A) Experimental selection of the microdevice's working frequency. The frequency sensitive metric is the ratio between the increase in impedance magnitude ($|Z_{certain\text{-}time}(f)|$-$|Z_{cell\text{-}free}(f)|$) and the impedance magnitude of the cell-free device $|Z_{cell\text{-}free}(f)|$. Error bar: standard deviation, n = 3 repeated independent measurements. (B) Representative experimental impedance waveforms, reflecting adhesion, spreading, and contractile behaviors of the hiPSC-CMs (electrode width = 40 μm for this particular device). Bottom-left inset shows impedance of hiPSC-CMs at the 24th hour. Top-left inset shows rhythmic contraction at the 36th hour, revealed simultaneously impedance spectroscopy and AFM. Top-right inset shows waveforms of impedance and contractile stress at 120th hour. (C) Relationship between contractile stress and the peak-to-peak value of impedance $|Z|_{p\text{-}p}$ per unit area. The grey region is the prediction intervals with a confidence level of 95%.

electrodes, producing a functional, beating 2D tissue monolayer. By recording electrical impedance signals, the device array monitored cell behavior at different phases, including adhesion, initiation of contraction, and plateaued contractility. The contractile stress was measured via atomic force microscopy (AFM), and quantitatively related to the electrical impedance signals. The established relationship was validated by comparing the changes to the AFM-measured and impedance-measured contractile stress after treatment with the L-type calcium channel blocker verapamil. Our quantitative power-law relationship between the contractile stress and impedance per unit electrode area expands the application of impedance measurement to the accurate quantification of cardiomyocyte contractile stress, facilitating the use of this label-free technique in the discovery of potential therapeutics for heart failure.

2. Results and discussion

2.1. Impedance and contractile stress measurement

We utilized an impedance spectrometer (HF2IS, Zurich Instruments) and a bio-AFM (AFM, Bioscope Catalyst, Bruker) for impedance and contractile stress measurement on iPSC-CMs. (Fig. 1B). While impedance signals were recorded, the AFM probe was moved onto the surface of a cardiomyocyte for simultaneous measurement of contractile stress.

The AFM measurement requires direct contact between the AFM probe and the cell. Indentation by the AFM probe can mechanically stimulate cardiomyocytes through stretch-induced activation of calcium channels or *area composita* (Pieperhoff et al., 2009; Moncayo-Arlandi and Brugada, 2017; Bers, 2002), with contact stress reported in the literature ranging from 3.1 kPa to 12.7 kPa (Ossola et al., 2015; Pesl et al., 2016; Smolyakov et al., 2017; Borin et al., 2020). To select an appropriate value for our measurement, indentation depths of 10 nm, 20 nm, 30 nm, and 40 nm were tested, as shown in Fig. 2A. When the tip-less AFM probe (nominal spring constant = 0.01 N/m, minimum 0.005 N/m, maximum 0.02 N/m) contacted the cardiomyocyte with an indentation depth of 10 nm, the contractile stress generated by individual iPSC-CMs were measured to be 9.52 ± 0.13 kPa (n = 9 cells, Fig. 2B). When the indentation depth was increased to 20 nm and 30 nm, the contractile stress was measured to be 9.58 ± 0.15 kPa (n = 9 cells) and 9.64 ± 0.29 kPa (n = 9 cells), respectively. However, the contractile stress dramatically increased to 12.77 ± 0.75 kPa when the indentation depth was increased to 40 nm ($P < 0.0001$ compared to10 nm, 20 nm, and 30 nm).

These results indicate that the application of a large force from the AFM probe on cardiomyocytes (0.4 nN, which corresponds to a 40 nm indentation depth) can undesirably cause the cell to generate significantly larger contractile stress, and that smaller indentation depths allow for AFM measurement without altering the inherent cell physiology. Thus, a small indentation depth of 10 nm was chosen for measurements of contractile stress, and the indentation depths larger than 40 nm were not tested for contractile stress measurement. The significant increase of contractile stress caused by 40 nm indentation may be attributed to the following reasons. (1) The large contact force (approximately 0.4 nN) may have activated the *area composita* of cardiomyocytes. Area composita are cadherin-mediated heart-muscle adhering junctions. Adhering junctions are connected via bipolar intercalated disks (IDs) that are responsible for cell adhesion and force transmission during heart muscle contraction (Pieperhoff et al., 2009). The activation of *area composita* has been shown to strengthen cardiomyocyte contraction (Moncayo-Arlandi and Brugada, 2017). (2) The large force can also potentially active Ca^{2+} channels on the cell membrane and cause Ca^{2+} influx into cells, leading to enhanced contraction due to the inherent excitation-contraction mechanism in cardiomyocytes (Bers, 2002).

A small indentation depth results in a small contact area between the AFM probe and the cell membrane (e.g., 23 μm^2 ± 2 μm^2 under the indentation depth of 10 nm). To study whether local measurement using a small contact area is representative of a cardiomyocyte monolayer, contractile stress measurements were obtained from geometrically distant cells (minimum 2 mm between measured cells), with the results shown in Fig. 2C. Using an indentation depth of 10 nm, the measured contractile stress ranged from 8.42 kPa to 10.71 kPa. While heterogeneity in cardiomyocyte activity is known to exists in a monolayer (Maltsev et al., 2004), our findings suggested a uniform generation of contractile stress (no statistical significance across the monolayer, 9.52 ± 0.13 kPa, n = 9 cells) using an indentation depth of 10 nm.

To determine if a quantitative relationship between impedance measurements and contractile stress exist, impedance spectrometric and AFM-determined contractile stress were recorded simultaneously. To determine the optimal working frequency for the microdevice, the frequency-dependence of the impedance signal was quantified (Fig. S1A), including at cell free stages and with cell monolayer creation (cell adhesion, spreading, and monolayer beating). The impedance magnitude varies with sampling frequency because the impedance generated by the capacitive components is frequency dependent (Fig. 1C and D). To select the optimal working frequency for the device, the frequency-sensitive metric (Pauwelyn et al., 2015; Qiu et al., 2008; Wegener et al., 2000b), i.e., the ratio between the increase in impedance magnitude ($|Z_{cultured\ time}(f)|$-$|Z_{cell\ free}(f)|$) and the impedance magnitude of the cell-free device ($|Z_{cell\ free}(f)|$) was used, where $|Z_{cultured\ time}(f)|$

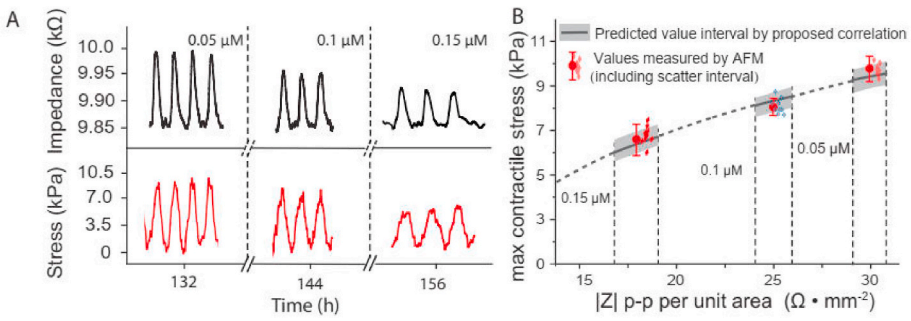

Fig. 4. (A) Tissue monolayer contractility measurements performed by impedance method (top) and AFM (bottom) during testing with increasing concentration of verapamil. (B) Comparison of contractile stress values measured by AFM and as predicated by our developed relationship between impedance and contractile stress (n = 3).

denotes the impedance magnitude of the cells at a specific time. The determined relationship between the frequency-sensitive metric and the device sampling frequency, by sweeping from 100 Hz to 100 kHz with a voltage magnitude of 650 mV, revealed that the optimal metric was obtained at 1 kHz frequency (Fig. 3A). Therefore, 1 kHz was selected as the working frequency.

Within 4 h of cell seeding, the magnitude of the impedance signal was observed to increase slightly and continued to increase over the next five days (Fig. 3B), before reaching a plateau. The initial increase of impedance magnitude was due to the attachment of cells to the electrodes, and the changes thereafter resulted from cell spreading, cell contraction and the establishment of tight intercellular contacts (facilitating coordinated 2D tissue contraction). Periodic waves of impedance signals became apparent after culturing for 36 h (top-left inset in Fig. 3B and Fig. S1E), indicating the appearance of rhythmic cardiomyocyte contraction. Although impedance magnitude increased slightly after culturing for 60 h, the peak-to-peak value of impedance waves ($|Z|_{p-p}$) plateaued after culturing for 120 h (Fig. S1 F-M, P value between the peak-to-peak value of impedance at 120th hour and that at 132nd hour $\geq$0.08). When the contraction of cardiomyocytes generated periodic impedance waveforms (after culturing for 36 h), AFM indentation for contractile stress measurement was performed every 12 h.

2.2. Relationship between contractile stress and impedance per unit electrode area

During impedance measurement, the electrodes were applied with alternating current of low magnitude (<10 mA) and high frequency (>400 Hz). The current flows along two paths, one extracellular and one transcellular (Fig. 1C). To better understand the two current paths, an equivalent circuit model was established. The model includes three impedance components, Z_{cell}, Z_{medium}, and $Z_{electrode}$, corresponding to the electrical impedance from the cell, the medium, and the electrode. Electric current passes through medium, cell, and electrode in series. The inter-cellular current is impeded by the resistance between adjacent cells (R_b); the trans-cellular current is impeded by the upper and lower plasma membrane (C_1 and C_2) and by the electrode in contact with the cell membrane (Z_{cw}).

According to (Giaever and Keese, 1991; Reiss and Wegener, 2015), the total impedance is

$$Z_{total} = \left[\frac{1}{Z_{electrode}} \left(\frac{Z_{electrode}}{Z_{electrode} + Z_{cell}} \right) + \frac{\frac{Z_{electrode}}{Z_{electrode}+Z_{cell}}}{0.5\gamma \frac{I_0(\gamma r_c)}{I_1(\gamma r_c)} + R_b \left(\frac{1}{Z_{electrode}} + \frac{1}{Z_{cell}} \right)} \right]^{-1} + Z_{medium} \quad (1)$$

where $I_0(\gamma r_c)$ and $I_1(\gamma r_c)$ denote modified Bessel functions of the first kind of order zero and one, respectively. Z_{total} represents the total impedance of the impedance measurement device with cells seeded; $Z_{electrode}$ is the impedance of a cell-free electrode; Z_{cell}represents the membrane capacitance of cardiomyocytes; Z_{medium} is the impedance of culture medium; R_b is the resistance between adjacent cells; and r is the effective radius of cardiomyocytes. In Eq. (1)

$$\gamma = \frac{Z_{cw}}{r_c} \sqrt{\frac{1}{Z_{electrode}} + \frac{1}{Z_{cell}}} \quad (2)$$

$$Z_{cw} = r_c \sqrt{\frac{\rho}{h}} \quad (3)$$

$$R_b = \rho \frac{r_c}{\pi (D - 2r_c)^2} \quad (4)$$

where r_c is resistivity of culture medium; h is the gap between electrode surface and cardiomyocyte; and D is the distance between adjacent cardiomyocytes.

The change in Z_{cell} is due to cardiomyocyte contraction, which alters cell morphology and effective contact area with electrodes. Contraction shortens the equivalent radius of the cells (r_c), resulting in an increase of each component (R_b, Z_c, and Z_{cw}) in Z_{cell} [Eqs. (2)–(4)].

$Z_{electrode}$ depends on the electrode material (Au) and geometry, and is fixed after the device is fabricated. To avoid the effect from the electrode geometry differences, normalized impedance $|Z|_{p-p}$ was calculated by dividing the magnitude of $Z_{electrode}$ by the electrode area S. Devices with different electrode geometries (electrode number, size etc.) are normalized by the electrode area S, i.e.,

$$|Z|_{p-p} = \frac{|Z_{electrode}|}{S} \quad (5)$$

The change in Z_{medium} is caused by inflow and outflow of various ions during cardiomyocyte contraction. Within the contractile cycle, sodium and calcium flow from culture medium into the cardiomyocyte, after which potassium flows from cardiomyocyte into culture medium (Bers, 2002). The flows of ions could affect the impedance of culture medium, Z_{medium}. However, since the change in sodium, potassium and calcium concentrations is small compared to the baseline concentration of the ions in the medium (baseline impedance in the cell-free condition is in the scale of 1 kΩ, as shown in see Fig. S1A), the change of Z_{medium} during cardiomyocyte contraction is small (in the scale of 10^{-6} kΩ, as measured by inserting two probes in the culture medium of beating cardiomyocytes) compared to the change of Z_{cell} during cardiomyocyte contraction (in the scale of 10^{-1} kΩ).

In summary, when cardiomyocytes contract and generate contractile stress, the shortened equivalent radii of the cells leads to an increase in R_b, Z_c, Z_{cw}, and Z_{cell}, while the impedance from the device is not affected by the cells' contractile stress. Therefore, changes to the overall impedance (Z_{total}) quantitatively reflect the contractile stress generated by the cells. We found that the experimentally quantified relationship between contractile stress and impedance per unit area satisfied a

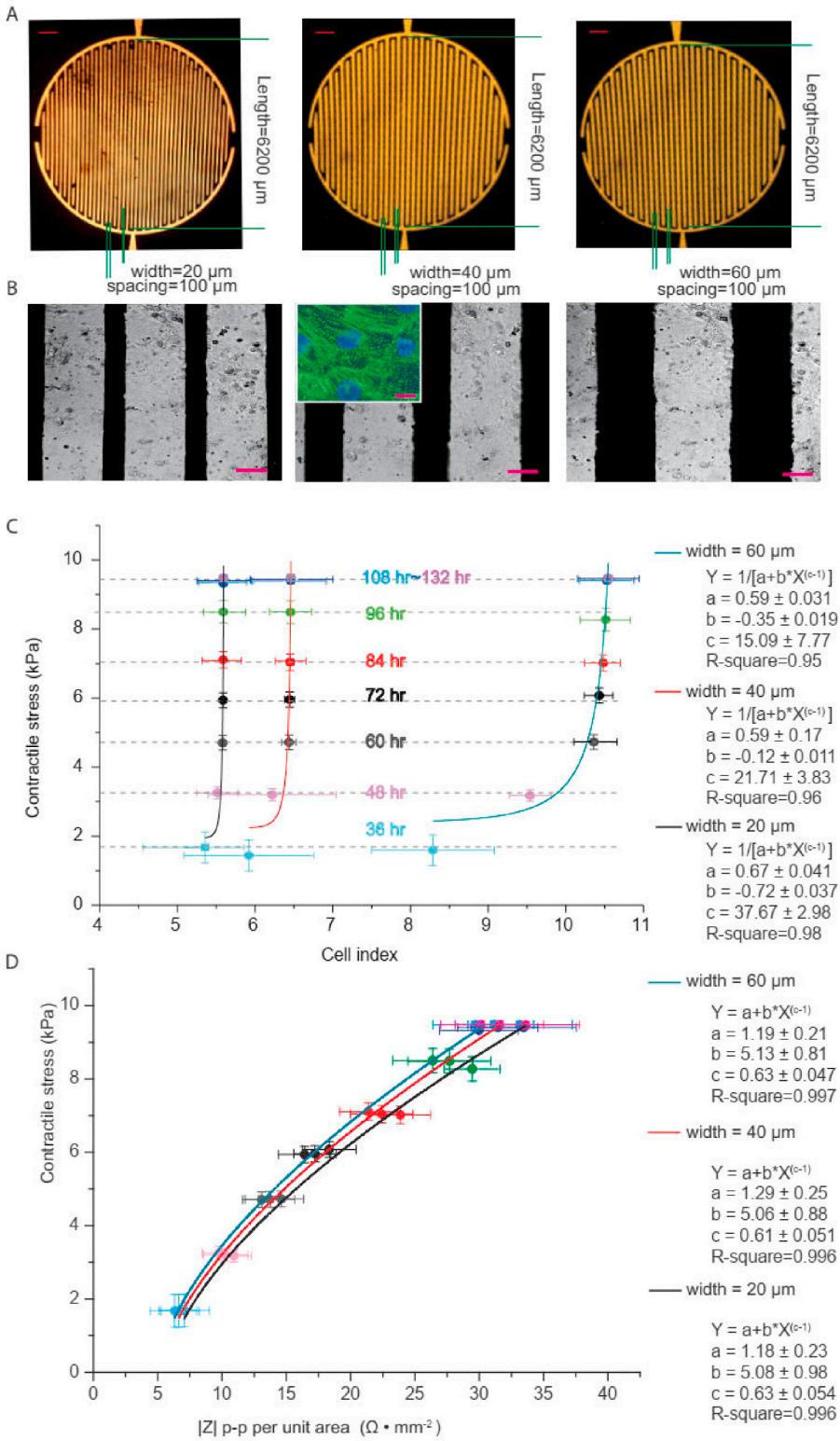

Fig. 5. (A) Devices created with different electrode geometries. (B) iPSC-CMs cultured on the devices (magnification 20×). Inset shows a confocal image of the cardiomyocytes on the device which formed a monolayer after culturing for 36 h, proving that the cells fully covered the device. Cells were fixed and stained: α-actinin (green) and nucleus (blue). Scale bar: 30 μm. (C) Traditional cell index vs. contractile stress for the three devices, at different culturing time points. (D) $|Z|_{p\text{-}p}$ per unit electrode area vs. contractile stress for the three devices, at different culturing time points. All follow the power-law relationship. (For interpretation of the references to colour in this figure legend, the reader is referred to the Web version of this article.)

power-law, Fig. 3C, with the largest contribution to model uncertainty from the variations in the cell morphology parameters of individual cardiomyocytes; for example, the cell height varied from 4.2 μm to 6.3 μm, and the cell spreading area varied from 3.89 μm^2 (Brette et al., 2017) to 5.77 μm^2 (Brette et al., 2017).

2.3. Validation of impedance-contractility relationship

To validate the quantified relationship between contractile stress and impedance, 2D iPSC-CM monolayers were treated with verapamil, an L-type calcium channel blocker that decreases contractility and beating rate by inhibiting Ca^{2+} transit (Tanaka et al., 2009). Three concentrations (0.05 μM, 0.1 μM, and 0.15 μM) of verapamil that represent

clinically relevant drug amounts were used to treat cardiomyocyte monolayers after culturing until stable beating (132 h). After verapamil treatment, the impedance signal was recorded and converted to contractile stress using the derived relationship, allowing for comparison to direct measurements performed with AFM (Fig. 4A). As expected, we observed a dose-dependent and linear decrease in the contractility measurements after the addition of verapamil. The contractile stress values as measured by AFM were 9.04 ± 0.14 kPa (0.05 μM), 7.72 ± 0.11 kPa (0.10 μM) and 6.23 ± 0.17 kPa (0.15 μM), and as predicted by impedance using the derived power-law relationship were 9.39 kPa, 7.76 kPa, and 6.05 kPa with a relative error of 3.73%, indicating no significance difference in the measurements between the techniques across the drug concentration series.

2.4. Dependence of measurements on electrode geometry

With existing impedance measurement methods, cell index ($|Z_x| - |Z_0|)/ |Z_0|$ has been used as a surrogate to reflect the contractility of cardiomyocytes, but the reported raw values of this metric can vary significantly (Xiao et al., 2010; Qiu et al., 2008; Qian et al., 2017) due to variations in electrode geometries adversely affecting the reproducibility and reliability of compound testing. The cell index is related to $|Z_0|$ (impedance magnitude of a cell-free device) that is electrode geometry-dependent (number, length, width, and spacing of interdigitated microelectrodes). To experimentally investigate the geometry dependence of our technique, devices with three different geometries of microelectrodes were used for culturing cardiomyocytes with the same cell density (Fig. 5, device 1: width = 20 μm, length = 6.2 mm, spacing = 100 μm, electrode area = 3.03 mm^2; device 2: width = 40 μm, length = 6.2 mm, spacing = 100 μm, electrode area = 5.19 mm^2; device 3: width = 60 μm, length = 6.2 mm, spacing = 100 μm, electrode area = 6.81 mm^2). Using the same iPSC-CM monolayer culture density and timing for all three devices, the impedance data was collected and traditional cell index values were calculated (Fig. 5C). At each culturing time point, representing different states of monolayer function (attachment, spreading, and coordinated contraction), the cell index values were statically different among the three devices. For instance, at the 96th hour, the cell index value was 5.51 ± 0.084 for the device with width = 20 μm, 6.33 ± 0.14 for the device with width = 40 μm, and 10.07 ± 0.18 for the device with width = 60 μm (ANOVA test, $P < 0.0001$). These results illustrate that if the traditional cell index is used for predicting contractile stress, electrode geometry dependency is significant, and devices with different electrode geometries must be individually calibrated in order for impedance to genuinely reflect contractile stress.

Alternatively, we use impedance per unit area to establish the relationship between contractile stress and impedance. The electrode number, length, and spacing together determine the effective area of electrodes, making impedance per unit area less geometry-dependent after normalization. As shown in Fig. 5D, the predicated contractile stress values using the quantified power-law relationship are consistent across all the tested geometrics device (P-values>0.91). The relationship between contractile stress and impedance per unit electrode area for the three different electrode geometries all followed the power-law form (vs. exponential-law form in Fig. 5C when a traditional cell index is used), with pair-wise P-values larger than 0.83 for all culturing time points.

3. Conclusion

Heat failure is the single largest cause of death in the developed countries, and possesses the largest individual treatment cost of any disease. Yet there is a paucity of pharmaceuticals that directly target the contractile defects of the cardiomyocyte, in part because of the difficulty in measuring this quantity accurately and over time in preclinical models. The continuous functional measurement of iPSC cardiomyocyte monolayers by electrical impedance provide an important label-free method for the evaluation of potential therapeutics using human-derived cells and tissue. We have addressed an important limitation of this method by describing how impedance measurements can be accurately and repeatable used to quantify tissue monolayer contractility. Our delivered method was validated using the commonly prescribed calcium channel blocker verapamil, known to alter human heart contractility. We illustrate how normalizing electrode area removes the dependence of contractile stress measurements on electrode geometry, with impedance and contractility following a power-law relationship across a large dynamics range a low error (less than 3.73%). Our findings will allow for the use of impedance measurements to repeatable quantify cardiomyocyte and cardiac tissue monolayer contractility, enabling label-free evaluation of new potential heart failure medications.

Declaration of competing interest

The authors declare that they have no known competing financial interests or personal relationships that could have appeared to influence the work reported in this paper.

CRediT authorship contribution statement

Xian Wang: Conceptualization, Methodology, Writing - original draft. **Li Wang:** Conceptualization, Methodology, Writing - original draft. **Wenkun Dou:** Methodology, Visualization, Validation. **Zongjie Huang:** Methodology, Visualization. **Qili Zhao:** Methodology, Visualization. **Manpreet Malhi:** Methodology. **Jason T. Maynes:** Supervision, Writing - review & editing. **Yu Sun:** Conceptualization, Supervision, Writing - original draft.

Acknowledgment

The authors acknowledge financial support from the Canadian Institutes of Health Research (CIHR) and the Natural Sciences and Engineering Research Council of Canada (NSERC); from the Explore Program of CQDM; and from the University of Toronto via an EMHSeed grant. L. W. acknowledges a postdoctoral fellowship from Ted Rogers Center for Heart Research Education Fund. Y.S. acknowledges the Canada Research Chairs Program. J.T.M. would like to thank the Wasser Family and SickKids Foundation, as the holder of the Wasser Chair in Anesthesia and Pain Medicine.

Appendix A. Supplementary data

Supplementary data to this article can be found online at https://doi.org/10.1016/j.bios.2020.112399.

Experimental Methods

Device Fabrication

Devices with three electrode dimensions (electrode width = 20 μm, 40 μm, and 80 μm) were fabricated. A glass substrate was rinsed by acetone, isopropanol, and deionized water. S1818 photoresist was spin-coated at 2000 rpm for 1 min, followed by UV exposure and development. The electrodes were formed by sputtering and lift-off, composed of a Cr layer with a thickness of 15 nm and an Au layer with a thickness of 150 nm.

Cell culture and drug treatment

Human induced pluripotent stem cell-derived cardiomyocytes (hiPSC-CMs) were obtained from Cellular Dynamics International. Prior to culturing, microdevices were UV sterilized. The sterilized top surface

of the devices was coated with a matrix mixture consisting of fibronectin, gelatin, and laminin and incubated at 37 °C for at least 4 h. Cells were plated at a density of 1.56×10^5 cells/cm^2 in iCell Cardiomyocyte Plating Medium (Cellular Dynamics International) and cultured at 37 °C/5% CO_2. Cells were thawed in hiPSC-CMs Plating Medium (Cellular Dynamics International) and centrifuged for 5 min at 180 g. After 4 h of post-plating, the plating medium was replaced with iCell Cardiomyocyte Maintenance medium, and the maintenance medium was subsequently replaced every second day. Once after hiPSC-CMs were seeded, the microdevice array was placed in a humidified 37 °C incubator with 5% CO_2, and the impedance signal started to be recorded. For testing the effect of verapamil (M5644, Sigma-Aldrich), 100 μL serum-free media was added to each well of the device array, and the dose of the drug was increased gradually by adding 1 μL more drug of higher concentration each time. After each drug addition, cells were incubated for 10 h for each dose before impedance signals were recorded.

Impedance and contractile stress measurement

To establish the relationship between impedance and the contractile stress of cardiomyocytes, an Atomic Force Microscopy, AFM (Bioscope Catalyst, Bruker) and an impedance spectroscope (HF2IS, Zurich Instruments) were used. The system was built around on an inverted fluorescent microscope (Nikon Eclipse TS100). Microscopy imaging provides visual feedback for AFM to locate the AFM Probe and cells. Each element in the microdevice array has a pair of electrodes including the working electrode and counter electrode. The pair of electrodes were connected to the impedance spectroscope. Impedance signal was continuously recorded; a tip-less AFM cantilever (MLCT-D, Bruker) with a spring constant of 0.01 N/m was used. The AFM tip was moved to a cardiomyocyte to obtain force-displacement curves around the cell center. Thirty two repeated measurements were collected for each cell, and statistics were calculated for the forces, intervals between beats, and duration of each contraction. Forces across cells were compared with two-tailed Student's t-test. Stress was obtained by dividing force with contact area.

References

Bers, D.M., 2002 Jan. Nature 415 (6868), 198–205.
Bildyug, N.B., Khaitlina, S.Y., 2019 Sep 1. Cell Tissue Biol. 13 (5), 360–365.
Borin, D., Peña, B., Chen, S.N., Long, C.S., Taylor, M.R., Mestroni, L., Sbaizero, O., 2020 Jan 1. Heliyon 6 (1), e03175.
Brette, F., Shiels, H.A., Galli, G.L., Cros, C., Incardona, J.P., Scholz, N.L., Block, B.A., 2017 Jan 31. Europe PMC 7 (1), 1–9.
Bürgel, S.C., Escobedo, C., Haandbæk, N., Hierlemann, A., 2015 Apr 1. Sens. Actuators, B 210, 82–90.
Fan, W., Chen, X., Ge, Y., Jin, Y., Jin, Q., Zhao, J., 2019 Dec 1. Biosens. Bioelectron. 145, 111730.
Gaitas, A., Malhotra, R., Li, T., Herron, T., Jalife, J., 2015 Mar 25. Rev. Sci. Instrum. 86 (3), 034302.
Giaever, I., Keese, C.R., 1984 Jun 1. Proc. Natl. Acad. Sci. U. S. A 81 (12), 3761–3764.
Giaever, I., Keese, C.R., 1991 Sep 1. Proc. Natl. Acad. Sci. U. S. A 88 (17), 7896–7900.
Gorski, P.A., Ceholski, D.K., Hajjar, R.J., 2015 Feb 3. Cell Metabol. 21 (2), 183–194.
Green, E.M., Wakimoto, H., Anderson, R.L., Evanchik, M.J., Gorham, J.M., Harrison, B. C., Henze, M., Kawas, R., Oslob, J.D., Rodriguez, H.M., Song, Y., 2016 Feb 5. Science 351 (6273), 617–621.
Hassanabad, A.F., MacQueen, K.T., Ali, I., 2019 Oct. J. Cardiothorac. Surg. 34 (10), 1075–1082.
Jacot, J.G., McCulloch, A.D., Omens, J.H., 2008 Oct 1. Biophys. J. 95 (7), 3479–3487.
Ke, N., Wang, X., Xu, X., Abassi, Y.A., 2011. Methods in Molecular Biology. Clifton, NJ vol. 740, 33–43.
Li, X., Zhang, R., Zhao, B., Lossin, C., Cao, Z., 2016 Aug 1. Arch. Toxicol. 90 (8), 1803–1816.
Liu, J., Sun, N., Bruce, M.A., Wu, J.C., Butte, M.J., 2012. PloS One 7 (5).
Maltsev, V.A., Vinogradova, T.M., Bogdanov, K.Y., Lakatta, E.G., Stern, M.D., 2004 Apr 1. Biophys. J. 86 (4), 2596–2605.
Moncayo-Arlandi, J., Brugada, R., 2017 Dec. Nat. Rev. Cardiol. 14 (12), 744.
Ossola, D., Amarouch, M.Y., Behr, P., Vörös, J., Abriel, H., Zambelli, T., 2015 Mar 11. Nano Lett. 15 (3), 1743–1750.
Pauwelyn, T., Reumers, V., Vanmeerbeeck, G., Stahl, R., Janssens, S., Lagae, L., Braeken, D., Lambrechts, A., Label-free cardiac contractility monitoring for drug screening applications based on compact high-speed lens-free imaging. In: Imaging, Manipulation, and Analysis of Biomolecules, Cells, and Tissues XIII 2015 Mar 2 (Vol. vol. 9328, p. 932818).
Pesl, M., Pribyl, J., Acimovic, I., Vilotic, A., Jelinkova, S., Salykin, A., Lacampagne, A., Dvorak, P., Meli, A.C., Skladal, P., Rotrekl, V., 2016 Nov 15. Biosens. Bioelectron. 85, 751–757.
Pieperhoff, S., Bennett, W., Farrell, A.P., 2009 Nov. J. Anat. 215 (5), 536–547.
Qian, F., Huang, C., Lin, Y.D., Ivanovskaya, A.N., O'Hara, T.J., Booth, R.H., Creek, C.J., Enright, H.A., Soscia, D.A., Belle, A.M., Liao, R., 2017. Lab Chip 17 (10), 1732–1739.
Qiu, Y., Liao, R., Zhang, X., 2008 Feb 15. Anal. Chem. 80 (4), 990–996.
Qiu, Y., Liao, R., Zhang, X., 2009. Preventing cardiomyocytes from TNF-α-induced cell death based on the impedance-sensing technique for real-time monitoring cell adhesion. In: In TRANSDUCERS 2009-2009 International Solid-State Sensors, Actuators and Microsystems Conference. IEEE, pp. 65–68.
Reiss, B., Wegener, J., 2015 Aug 25. Impedance analysis of different cell monolayers grown on gold-film electrodes. In: 37th Annual International Conference of the IEEE Engineering in Medicine and Biology Society, pp. 7079–7082.
Ribeiro, M.C., Slaats, R.H., Schwach, V., Rivera-Arbelaez, J.M., Tertoolen, L.G., Van Meer, B.J., Molenaar, R., Mummery, C.L., Claessens, M.M., Passier, R., 2020 Mar 20. J. Mol. Cell. Cardiol. 7079–7082.
Rudolph, F., Hüttemeister, J., da Silva Lopes, K., Jüttner, R., Yu, L., Bergmann, N., Friedrich, D., Preibisch, S., Wagner, E., Lehnart, S.E., Gregorio, C.C., 2019 Dec 10. Proc. Natl. Acad. Sci. U. S. A 116 (50), 25126–25136.
Sant Anna, R.T., Eibel, B., Markoski, M.M., Rodrigues, C.G., De Salles, F.B., Giusti, I.I., Nesralla, I.A., Nardi, N.B., Kalil, R.A., 2020. Gene Ther. 27 (1), 40–50.
Scott, C.W., Zhang, X., Abi-Gerges, N., Lamore, S.D., Abassi, Y.A., Peters, M.F., 2014 Dec 1. Toxicol. Sci. 142 (2), 331–338.
Skwarek-Maruszewska, A., Hotulainen, P., Mattila, P.K., Lappalainen, P., 2009 Jun 15. J. Cell Sci. 122 (12), 2119–2126.
Smolyakov, G., Cauquil, M., Séverac, C., Lachaize, V., Guilbeau-Frugier, C., Senard, J.M., Galés, C., Dague, E., 2017 Apr 1. J. Struct. Biol. 198 (1), 28–37.
Tanaka, T., Tohyama, S., Murata, M., Nomura, F., Kaneko, T., Chen, H., Hattori, F., Egashira, T., Seki, T., Ohno, Y., Koshimizu, U., 2009 Aug 7. Biochem. Biophys. Res. Commun. 385 (4), 497–502.
Tsai, S.L., Wang, M.H., 2016 Jun 28. Sens. Actuators, B 229, 225–231.
Wang, T., Hu, N., Cao, J., Wu, J., Su, K., Wang, P., 2013 Nov 15. Biosens. Bioelectron. 49, 9–13.
Wegener, J., Keese, C.R., Giaever, I., 2000 Aug 25. Exp. Cell Res. 259 (1), 158–166.
Wegener, J., Keese, C.R., Giaever, I., 2000 Aug 25. Exp. Cell Res. 259 (1), 158–166.
Xiao, L., Hu, Z., Zhang, W., Wu, C., Yu, H., Wang, P., 2010 Dec 15. Biosens. Bioelectron. 26 (4), 1493–1499.
Zhou, Y., Basu, S., Laue, E., Seshia, A.A., 2016 Jul 15. Biosens. Bioelectron. 81, 249–258.